FEBS Letters 581 (2007) 5178–5184

Appropriate expression of imprinted genes on mouse chromosome 12 extends development of bi-maternal embryos to term

Manabu Kawahara[a], Qiong Wu[a,1], Anne C. Ferguson-Smith[b], Tomohiro Kono[a,*]

[a] Department of BioScience, Tokyo University of Agriculture, Setagaya-ku, Tokyo 156-8502, Japan
[b] Department of Physiology, Development and Neuroscience, University of Cambridge, Downing Street, Cambridge CB2 3DY, UK

Received 13 August 2007; revised 25 September 2007; accepted 1 October 2007

Available online 12 October 2007

Edited by Ned Mantei

Abstract **Recently, we reported that the restored regulation of imprinted gene expression from two regions – *H19* differentially methylated region (*H19*-DMR) and intergenic germline-derived DMR (IG-DMR) – is sufficient for accomplishing full-term development in mice. In the present study, we determined the developmental ability of the bi-maternal embryos (BMEs) containing the non-growing oocyte genome with the IG-DMR deletion ($ng^{\Delta ch12}$) and fully-grown (fg) oocyte genome. Foetuses derived from $ng^{\Delta ch12}$/fg BMEs were alive at E19.5 but could not survive further. Comparison with BMEs derived from *Igf2*+/− ng/fg genomes suggests that bi-allelic *H19* expression might be involved in foetal development.**

Keywords: H19; Igf2; Genomic imprinting; Development; Mouse

1. Introduction

Genomic imprinting regulates the expression of developmentally crucial mammalian genes. Androgenetic and parthenogenetic embryos fail to develop past early post-implantation and mid-gestation, respectively, and disruption of imprinting is implicated in serious human diseases such as Angelman syndrome, Prader–Willi syndrome, Beckwith–Wiedemann syndrome and Silver–Russell syndrome [1–3]. Most imprinted genes are located in clusters, and each imprinted cluster is regulated by an imprint control region (ICR). Parental-specific DNA methylation marks that regulate the mono-allelic expression of imprinted genes are globally and accurately reprogrammed during either spermatogenesis or oogenesis [4].

In our previous work, we assessed the development of bi-maternal embryos (BMEs) consisting of two sets of haploid maternal genome from fully-grown (fg) and non-growing (ng) oocytes. Maternal methylation imprints had been acquired as normal, in the fg oocyte genome, while imprints had been erased but maternal methylation had not yet been acquired in the ng oocytes [5]. Because of this, unlike in parthenogenetic and gynogenetic embryos, BMEs can express the normally paternally expressed imprinted genes such as *Peg1/Mest*, *Peg3*, *Impact* and *Peg10*, resulting in extended development of the embryos to E13.5 [6,7]. Therefore, investigating the development of ng/fg BMEs that do not receive a contribution from the paternal genome is a powerful means of determining the paternal contribution to descendants.

It is known that the deletion of the intergenic germline-derived differentially methylated region (IG-DMR) from maternally inherited chromosome 12 leads to loss of imprinting of all genes in the 1-Mb cluster that carries the maternally repressed genes *Dlk1*, *Dio3* and *Rtl1*; and the maternally expressed non-coding RNAs, including *Gtl2*, and microRNAs. Hence the IG-DMR is the imprinting control region for this cluster of imprinted genes. This IG-DMR deletion from the maternally inherited chromosome results in lethality in mutant mice [8]. In contrast, the paternally methylated imprinted genes *Igf2* and *H19* present on chromosome 7 do not appear to be essential for foetal viability, since loss of paternal methylation imprinting by *H19*-DMR deletion did not result in lethality in mice [9,10]. These results appear to indicate that for foetal viability, paternal methylation imprinting on chromosome 12 is more important than that on chromosome 7.

To address this issue, we investigated the developmental ability of $ng^{\Delta ch12}$/fg BMEs in which the maternal unmethylated status of *H19*-DMR of the *Igf2–H19* locus on both maternal chromosomes would likely be maintained, although the methylation status of *H19*-DMR was not evaluated (Fig. 1). In addition, we performed quantitative gene expression analysis and histological analysis. As expected, the expression levels of *Dlk1*, *Gtl2*, *Dio3* and *Mirg* mRNAs in $ng^{\Delta ch12}$/fg BMEs were similar to those in wild-type foetuses at E18.5. In contrast, as expected, the expression levels of *Igf2* and *H19* mRNAs were repressed and overexpressed, respectively. By restoration of the expression of paternally methylated imprinted genes on chromosome 12, we found that the $ng^{\Delta ch12}$/fg BMEs could develop to E19.5 but showed severe growth retardation as compared to the wt foetuses and the $ng^{\Delta ch7}$/fg BMEs. Furthermore, $ng^{\Delta ch12}$/fg BMEs did not show normal respiration and development after birth, which was observed in $ng^{\Delta ch7}$/fg BMEs. Histological evaluation of the lungs of $ng^{\Delta ch12}$/fg BMEs revealed thick alveolar septae and poorly organized alveoli. Our results allow comparison between the phenotypes of $ng^{\Delta ch7}$/fg and $ng^{\Delta ch12}$/fg conceptuses and provide insights into the relative contribution of imprinted genes on those chromosomes to development.

*Corresponding author. Fax: +81 3 5477 2543.
E-mail address: tomohiro@nodai.ac.jp (T. Kono).
[1]Present address: Department of Life Science and Engineering, Harbin Institute of Technology, No. 92, West Da-Zhi Street, Harbin, Heilongjiang, China.

0014-5793/$32.00
doi:10.1016/j.febslet.2007.10.004

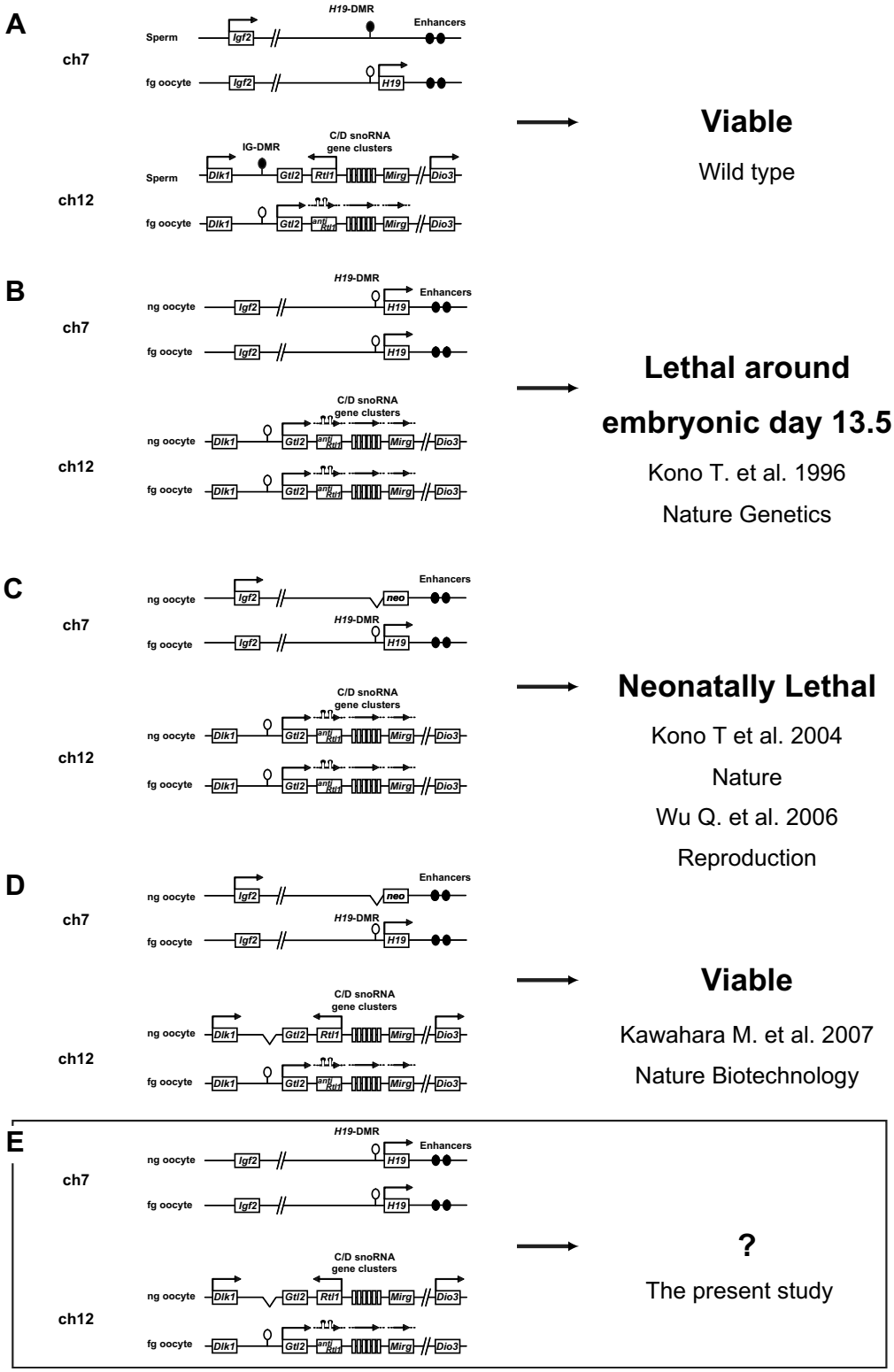

Fig. 1. Effect of predicted expression pattern of paternally methylated imprinted genes on chromosomes 7 and 12 on mouse viability: (A) wild-type (wt) bi-parental embryos, (B) ng^{wt}/fg bi-maternal embryos (BMEs), (C) $ng^{\Delta ch7}$/fg BMEs, (D) $ng^{\Delta DOuble}$/fg BMEs and (E) $ng^{\Delta ch12}$/fg BMEs.

2. Materials and methods

2.1. Serial nuclear transfer

Nuclear transfer was performed using a previously described method [5]. In brief, fully-grown germinal vesicle (GV) oocytes were placed in M2 medium after being collected from ovarian follicles of B6D2F1 (C57BL/6N × DBA) female mice 44–48 h after they were injected with equine chorionic gonadotrophin. Ovulated MII oocytes were also collected from superovulated B6D2F1 mice 16 h after they were injected with human chorionic gonadotrophin. We collected ng oocytes at the diplotene stage of the first meiosis from the ovaries of 1-day-old newborn mice derived from IG-DMRΔ4.5 heterozygous mutants.

Throughout the experiment, the GV oocytes were manipulated in M2 medium containing 200 μM dbcAMP and 5% calf serum. The ng oocytes were fused with enucleated GV oocytes by using inactivated Sendai virus (HVJ; 2700 haemagglutinating activity units/ml). The reconstructed oocytes were cultured for 14 h in α-MEM medium (GIBCO, Grand Island, NY) containing 5% calf serum. A spindle from the reconstructed oocytes was again transferred into the ovulated MII oocytes, followed by treatment with 10 mM $SrCl_2$ in Ca^{2+}-free M16 medium for 2 h. These embryos were cultured in M16 medium for 3.5 days in an atmosphere of 5% CO_2, 5% O_2 and 90% N_2 at 37 °C. Embryos that developed to the blastocyst stage were transferred into the uterine horns of recipient female mice at 2.5 days of pseudopregnancy. As the controls for (BMEs), wild-types were produced by mating between B6D2F1 females and C57BL/6N males.

2.2. Quantitative gene expression analysis

Using RNeasy Mini Kit (QIAGEN K.K., Tokyo, Japan), total RNA was extracted from the respective organs (brain, tongue, lung, heart, liver and kidney) of wt (B6D2F1 × C57BL/6N) foetuses and bi-maternal $ng^{\Delta ch7}$/fg and $ng^{\Delta ch12}$/fg BMEs at E18.5. The cDNAs were then synthesized using the SuperScript™III RNaseH-reverse Transcriptase kit (Invitrogen, Carlsbad, CA), cDNAs were synthesized in a reaction solution (20 μl) containing the total RNA (1 μg) obtained from each foetus. Finally, we performed a quantitative analysis of gene expression by using real-time PCR (7500 Real-Time PCR System; SYBR® GREEN PCR Master Mix Applied Biosystems). The primers used for the analysis were as described in our previous study [11].

2.3. Histological analysis

Live foetuses at 19.5 days of gestation derived from wt embryos and $ng^{\Delta ch7}$/fg and $ng^{\Delta ch12}$/fg BMEs were fixed with 4% paraformaldehyde and processed for wax embedding. Serial cross-sections were mounted on slides and stained with hematoxylin and eosin (H&E).

2.4. Statistical analysis

Statistical analyses of all data to be compared were carried out by one-way analysis of variance (ANOVA) and Fisher PLSD test using the software Statview (Abacus Concepts Inc., Berkeley, CA). A P value of <0.05 was considered significant.

3. Results

3.1. Developmental ability of the $ng^{\Delta ch12}$/fg BMEs

For developmental assessment, 397 blastocysts derived from $ng^{\Delta ch12}$/fg BMEs were transferred into the uterine horns of recipient female mice. Since ng^{wt}/fg BMEs can develop up to 13.5 days of gestation [5], autopsies to assess post-implantation development were carried out at 15.5, 18.5 and 19.5 days of gestation. At E18.5, seven live foetuses were recovered from 81 transferred embryos (Table 1). Furthermore, even at E19.5, five live foetuses could be recovered from 253 transferred embryos (Table 1). However, during gestation the weight of $ng^{\Delta ch12}$/fg BMEs was significantly less than that of wt foetuses (Fig. 2A). At E19.5, we found that $ng^{\Delta ch12}$/fg BMEs were alive, but their body weight was less than that of wt foetuses (<55%; Fig. 2B). Furthermore, $ng^{\Delta ch12}$/fg BMEs could not survive further due to failure of normal respiration, suggesting difficulty in full-term development.

Table 1
Development of $ng^{\Delta ch12}$/fg bi-maternal embryos

Developmental progress	
Number of embryos transferred	63
Number of implantations in recipients	54 (85.7%)
Alive at E15.5	10 (15.9%)
Number of embryos transferred	81
Number of implantations in recipients	66 (81.5%)
Alive at E18.5	7 (8.6%)
Number of embryos transferred	253
Number of implantations in recipients	204 (80.6%)
Dead	29 (11.5%)
Alive at E19.5	5 (2.0%)

The percentages in parentheses represent the proportions to transferred embryos.

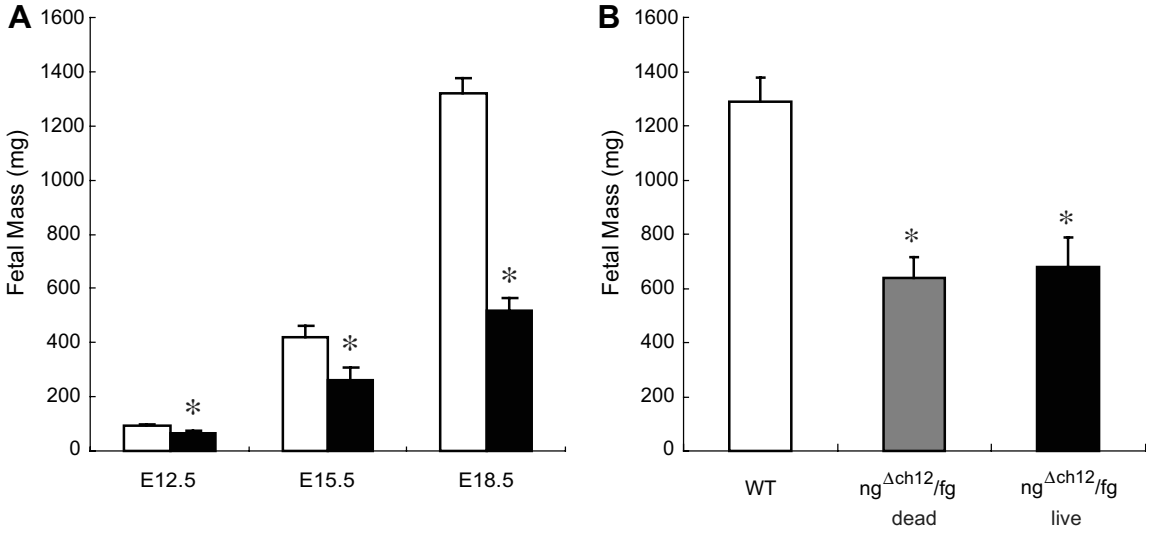

Fig. 2. Body weights of $ng^{\Delta ch12}$/fg BMEs during gestation and at E19.5: (A) the graph shows the body weights of wt bi-parental (white) and the $ng^{\Delta ch12}$/fg bi-maternal (black) foetuses at E12.5 (wt: $n = 4$, $ng^{\Delta ch12}$/fg: n = 6), E15.5 (wt: $n = 10$, $ng^{\Delta ch12}$/fg: $n = 3$) and E18.5 (wt: $n = 5$, $ng^{\Delta ch12}$/fg: $n = 5$) and (B) the graph shows the body weights of wt bi-parental fetuses (white) and the $ng^{\Delta ch12}$/fg bi-maternal dead (grey) and live (black) foetuses at E19.5 (wt: $n = 9$, dead BME: $n = 26$, live BME: $n = 5$). Dead fetuses did not show vital reaction at birth. * Significant differences for wt foetuses ($P < 0.05$).

3.2. Quantitative gene expression analysis of paternally methylated imprinted genes in $ng^{\Delta ch12}$/fg BMEs

To gain further insight into the mechanism underlying the extended development and neonatal lethality of the $ng^{\Delta ch12}$/fg BMEs, quantitative expression analysis was performed in individual $ng^{\Delta ch12}$/fg BMEs by using quantitative real-time PCR. At E18.5, the *Igf2* level in these foetuses was repressed in most tissues, except the brain (Fig. 3A). *H19* overexpression was observed in all tissues of $ng^{\Delta ch12}$/fg BMEs in which both maternal alleles were active, except for tongue and liver (Fig. 3B). This confirms that normal imprinting was not evident at this domain and that *H19* overexpression and *Igf2* underexpression most likely contributes to the significantly lower weight of $ng^{\Delta ch12}$/fg BMEs. In contrast, the expression

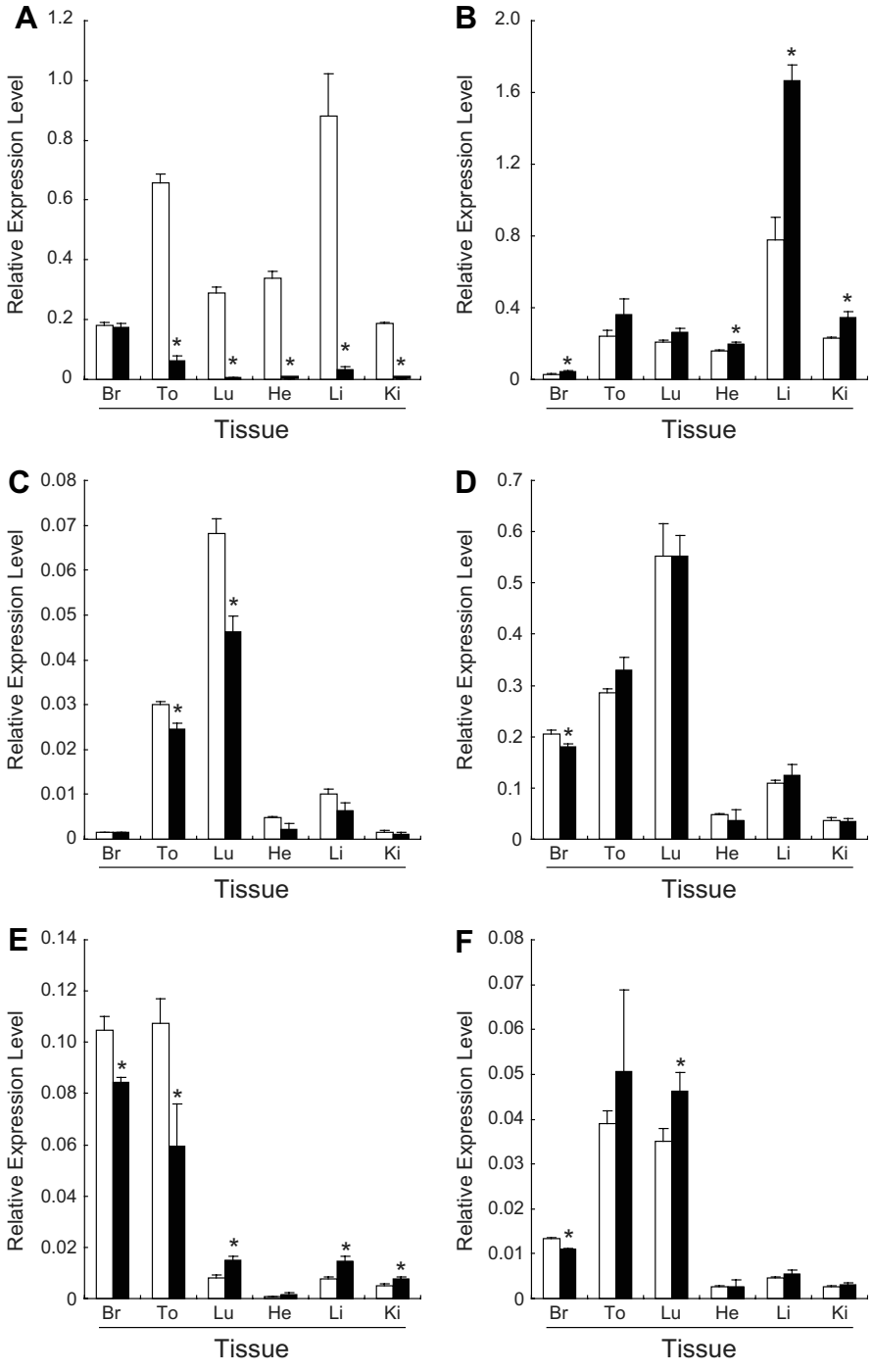

Fig. 3. Graphical representations of the expression of the two sets of imprinted genes in bi-maternal foetuses. The expression of six imprinted genes *Igf2* (A), *H19* (B), *Dlk1* (C), *Gtl2*(D), *Dio3* (E) and *Mirg* (F), in six different tissues obtained from foetuses at E18.5 were analysed by quantitative real-time PCR ($n = 3$). Br, brain; To, tongue; Lu, lung; He, heart; Li, liver and Ki, kidney. The values represent the levels of expression relative to that of the internal control gene (Gapdh). Wt ($n = 3$, white); $ng^{\Delta ch12}$/fg bi-maternal ($n = 3$, black). The values represent the means ± S.E.M. values. * significant differences for wt foetuses ($P < 0.05$).

of *Dlk1*, *Gtl2* and *Mirg* of ng$^{\Delta ch12}$/fg BMEs was obviously recovered in the most tissues, although the expression was still significantly different in some cases (Fig. 3C–E). Meanwhile, the expression levels of *Dio3* in ng$^{\Delta ch12}$/fg BMEs were found to be upregulated in brain and tongue, and downregulated in lung, liver and kidney as compared with wt foetuses (Fig. 3F).

3.3. Histological evaluation of respiratory organs of the wt foetus and of the ng$^{\Delta ch7}$/fg and ng$^{\Delta ch12}$/fg BMEs at E19.5

To gain further insight into the phenotypical anomalies in the BMEs, we performed histological analysis of the lungs and diaphragms of wt foetus, ng$^{\Delta ch7}$/fg and ng$^{\Delta ch12}$/fg BMEs at E19.5. In the present study, we compared the H&E-stained paraffin-embedded sections of the respiratory organs of all three types of foetuses since the histological evaluation of the ng$^{\Delta ch7}$/fg BMEs had not been subjected to histological analysis in the previous study [12].

The lungs of both ng$^{\Delta ch7}$/fg and ng$^{\Delta ch12}$/fg BMEs were atrophic and had severe anomalies (Fig. 4). When compared with wt foetuses, ng$^{\Delta ch7}$/fg and ng$^{\Delta ch12}$/fg BMEs showed thicker alveolar septae and poorly organized alveoli. However, the severity of lung defects in ng$^{\Delta ch12}$/fg BMEs was greater than that in ng$^{\Delta ch7}$/fg BMEs, and is most likely due to the absence of *Igf2* mRNA expression. Anomalies in the lungs of *Igf2* null foetuses have been described previously [13]. Next, we compared the diaphragms of the wt foetuses with those of ng$^{\Delta ch7}$/fg and ng$^{\Delta ch12}$/fg BMEs, because studies on mice with uniparental disomy for chromosome 12 suggested that the imprinted genes on chromosome 12 were associated with abnormalities in muscle development including in the diaphragm [14]. Diaphragms of ng$^{\Delta ch7}$/fg BMEs had significantly reduced thickness in the cross-sectional area compared to wild-type (81.4 ± 8.2 μm vs. 109.8 ± 6.9 μm, respectively; $n = 3$ for both, $P < 0.05$), although ng$^{\Delta ch12}$/fg BMEs (103.2 ± 11.0 μm, $n = 3$) did not. The contribution of the diaphragm hypotrophy to difficulties in breathing is not known.

4. Discussion

In the present study, by using ng oocytes of mice heterozygously carrying a 4.15-kb deletion of the IG-DMR on chromosome 12 (ng$^{\Delta ch12}$), we investigated the developmental ability of ng$^{\Delta ch12}$/fg BMEs in which the maternal methylation status of *H19*-DMR of the *Igf2–H19* locus in both alleles would likely be maintained.

The results of quantitative gene expression analysis demonstrated that in ng$^{\Delta ch12}$/fg BMEs, the imprinting status in the

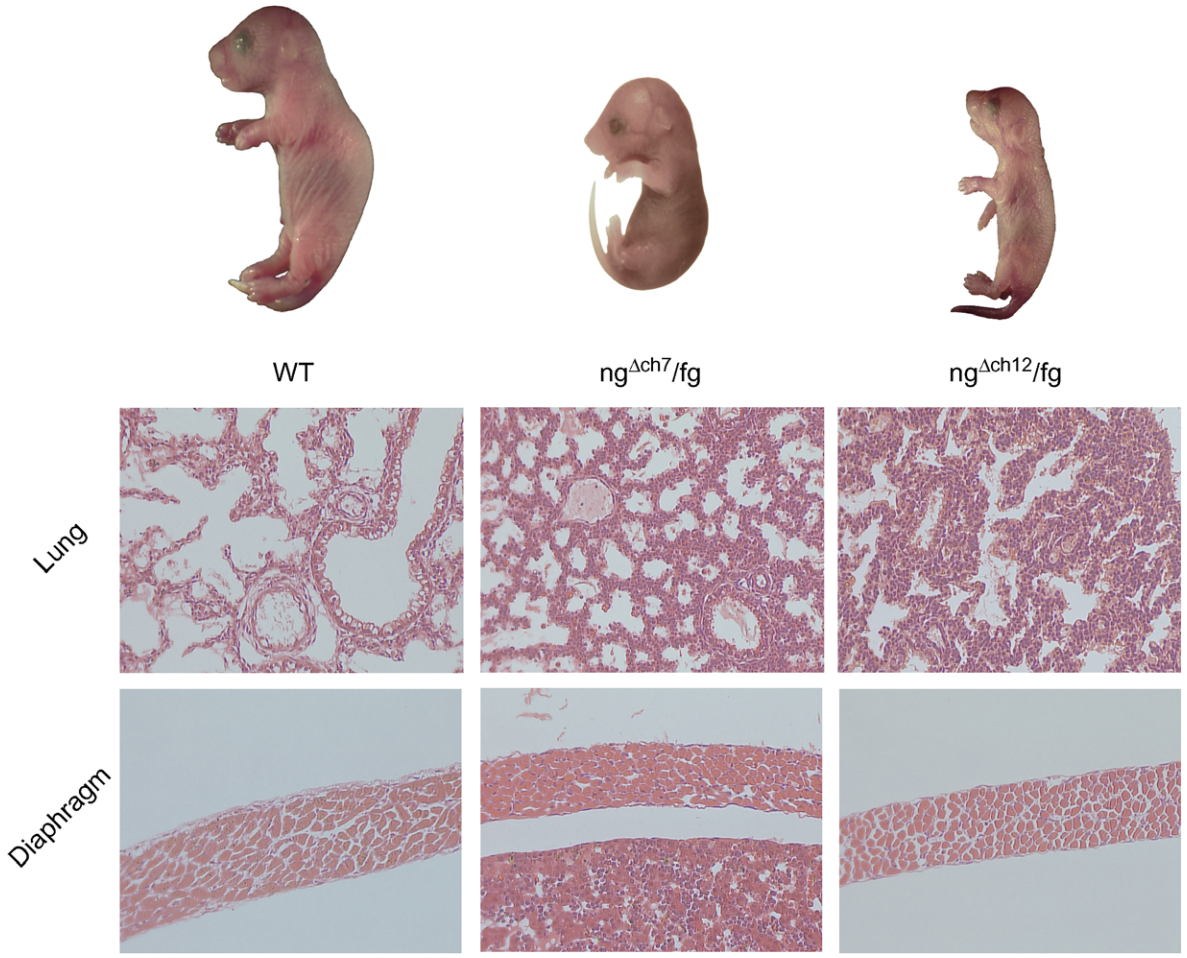

Fig. 4. Histological evaluation of lungs and diaphragm in wt foetuses, ng$^{\Delta ch7}$/fg and ng$^{\Delta ch12}$/fg BMEs at E19.5. Note that lungs obtained from ng$^{\Delta ch7}$/fg and ng$^{\Delta ch12}$/fg BMEs show thicker alveolar septae and poorly organized alveoli when compared with those of wt foetuses.

Igf2-H19 domain was disrupted, while the expression pattern of imprinted genes in the *Dlk1-Dio3* domain was consistent in principle with that in the wt foetuses with a few exceptions. ng$^{\Delta ch12}$/fg BMEs could develop beyond E15.5 and even up to E19.5. However, they had lower body weight than the wt foetuses (<55%). Disruption of the paternal allele of the imprinted embryonic gene coding for insulin-like growth factor 2 (IGF2; *Igf2*$^{+m/-p}$) results in viable mice whose weight is 60% of that of the wt littermates. This growth retardation in *Igf2*$^{+m/-p}$ mice is similar to that observed in ng$^{\Delta ch12}$/fg BMEs in this study. The weights of *Igf2*−/− embryos (inbred129/SvJ) at E16.5 and P1.5 were 311 mg and 620 mg, respectively [15]. Meanwhile, in the present study, the weights of ng$^{\Delta ch12}$/fg BMEs (B6D2F1 × C57BL/6N) were 258 mg and 680 mg at E15.5 and E19.5, respectively. These data indicate that the body weights from E15.5 to E19.5 are comparable between *Igf2*−/− mutants and ng$^{\Delta ch12}$/fg BMEs. IGF2 plays a role in cell cycle progression, and it is thought that one of the reasons why *Igf2* mutants are born smaller than normal is because of reduced cell proliferation [16]. *Igf2* deficiency appears to be responsible for the growth retardation in ng$^{\Delta ch12}$/fg BMEs.

Furthermore, histological analysis revealed that ng$^{\Delta ch12}$/fg BMEs had atrophic lungs with thicker alveolar septae and poorly organized alveoli, as observed in *Igf2* null mice [13]. It is known that *Igf2* plays an important role in the development of the foetal lung. However, ng$^{\Delta ch7}$/fg BMEs expressing *Igf2* mRNA also had aberrant lungs with thick alveolar septae, although the defects were milder than those in ng$^{\Delta ch12}$/fg BMEs. This indicated that paternally methylated imprinted genes on the *Dlk1–Dio3* domain also are involved in foetal lung development. *Dlk1*, *Rtl1* and *Dio3* are the three protein-coding genes on the *Dlk1–Dio3* domain. *Dlk1* encodes a transmembrane protein belonging to the Notch/Delta family of signalling molecules, and plays many roles in the differentiation of several tissues. Expression of *Dlk1* mRNA and protein is present during lung development however its function in that organ remains unclear [17,18].

Phenotypical characteristics of ng$^{\Delta ch12}$/fg BMEs were reminiscent of bi-parental embryos with deletion of the *Igf2* locus inherited from the paternal allele. However, there is a critical difference between the ng$^{\Delta ch12}$/fg BME and the *Igf2*$^{+m/-p}$ bi-parental mice; ng$^{\Delta ch12}$/fg BMEs showed neonatal lethality, whereas the *Igf2*$^{+m/-p}$ bi-parental mice were viable after birth. Some kind of synergistic effect of paternally methylated imprinted genes on chromosomes 7 and 12 might be involved in neonatal lethality of ng$^{\Delta ch12}$/fg BMEs. Alternatively, disrupted regulation of *H19* gene expression might be responsible for the neonatal lethality of ng$^{\Delta ch12}$/fg BME which retain the bi-allelic maternal methylation status of *Igf2–H19* ICR on chromosome 7. However, the *H19* gene function remains a matter of debate. It has been described as a putative suppressor gene; for example, *H19* mRNA expression in embryonal tumour cell lines could inhibit their growth and tumour-forming potential [19,20]. Furthermore, it has been demonstrated that *H19* gene expression might be involved in muscle cell differentiation during mouse development [21,22]. Several studies have been conducted to understand the biological function of *H19* mRNA by using mutant mice harbouring the deletion of *H19* transcription unit [23] and overexpressing *H19* mRNA [24]. Results have been inconsistent and include the finding that no obvious phenotype was detected from the altered gene dosage of *H19*. Meanwhile, bi-allelic *H19* expression in ng$^{\Delta ch12}$/fg BMEs would be a major difference in imprinted gene expression when compared with the *Igf2*$^{+m/-p}$ bi-parental mice. The present results do suggest that *H19* is involved in the developmental defects, although further studies are required to confirm this. Furthermore, abnormal placentation in ng$^{\Delta ch12}$/fg BMEs might be associated with their growth retardation and lethality, since ng$^{\Delta ch12}$/fg placentae showed reduced mass that could contribute to malnutrition during gestation [25]. Most recently, we constructed ng$^{\Delta Double}$/fg BMEs by using ng oocytes derived from double-knockout mice (ΔDouble) harbouring deletions in both the *H19*-DMR and the IG-DMR, which appropriately expressed paternally methylated imprinted genes on chromosomes 7 and 12 [11]. Surprisingly, ng$^{\Delta Double}$/fg BMEs survived to viable adult females with a high success rate equivalent to the rate observed with in vitro fertilization of manipulated normal embryos. Taken together, the present study shows that bi-allelic *H19* expression would be involved in lethality of ng$^{\Delta ch12}$/fg BMEs, suggesting that *H19* transcripts play some roles in mouse development.

Acknowledgements: We thank Dr. Shirley Tilghman, Princeton University for the gift of mutant mice. This work was supported by Grants from the Bio-oriented Technology Research Advancement Institution (BRAIN) of Japan, the Ministry of Education, Science, Culture and Sports of Japan, and the UK BBSRC.6.

References

[1] Weksberg, R., Smith, A.C., Squire, J. and Sadowski, P. (2003) Beckwith–Wiedemann syndrome demonstrates a role for epigenetic control of normal development. Hum. Mol. Genet. 12 (Spec No. 1), R61–R68.
[2] Nicholls, R.D. and Knepper, J.L. (2001) Genome organization, function, and imprinting in Prader–Willi and Angelman syndromes. Annu. Rev. Genomics Hum. Genet. 2, 153–175.
[3] Hitchins, M.P., Stanier, P., Preece, M.A. and Moore, G.E. (2001) Silver–Russell syndrome: a dissection of the genetic aetiology and candidate chromosomal regions. J. Med. Genet. 38, 810–819.
[4] Morgan, H.D., Santos, F., Green, K., Dean, W. and Reik, W. (2005) Epigenetic reprogramming in mammals. Hum. Mol. Genet. 14 (Spec No. 1), R47–R58.
[5] Kono, T., Obata, Y., Yoshimzu, T., Nakahara, T. and Carroll, J. (1996) Epigenetic modifications during oocyte growth correlates with extended parthenogenetic development in the mouse. Nat. Genet. 13, 91–94.
[6] Ogawa, H., Wu, Q., Komiyama, J., Obata, Y. and Kono, T. (2006) Disruption of parental-specific expression of imprinted genes in uniparental fetuses. FEBS Lett. 580, 5377–5384.
[7] Obata, Y. et al. (1998) Disruption of primary imprinting during oocyte growth leads to the modified expression of imprinted genes during embryogenesis. Development 125, 1553–1560.
[8] Lin, S.P., Youngson, N., Takada, S., Seitz, H., Reik, W., Paulsen, M., Cavaille, J. and Ferguson-Smith, A.C. (2003) Asymmetric regulation of imprinting on the maternal and paternal chromosomes at the Dlk1-Gtl2 imprinted cluster on mouse chromosome 12. Nat. Genet. 35, 97–102.
[9] Leighton, P.A., Ingram, R.S., Eggenschwiler, J., Efstratiadis, A. and Tilghman, S.M. (1995) Disruption of imprinting caused by deletion of the H19 gene region in mice. Nature 375, 34–39.
[10] Thorvaldsen, J.L., Duran, K.L. and Bartolomei, M.S. (1998) Deletion of the H19 differentially methylated domain results in loss of imprinted expression of H19 and Igf2. Genes Dev. 12, 3693–3702.
[11] Kawahara, M., Wu, Q., Takahashi, N., Morita, S., Yamada, K., Ito, M., Ferguson-Smith, A.C. and Kono, T. (2007) High frequency generation of viable mice from engineered bi-maternal embryos. Nat. Biotechnol. 25, 1045–1050.
[12] Kono, T. et al. (2004) Birth of parthenogenetic mice that can develop to adulthood. Nature 428, 860–864.

[13] Silva, D., Venihaki, M., Guo, W.H. and Lopez, M.F. (2006) Igf2 deficiency results in delayed lung development at the end of gestation. Endocrinology 147, 5584–5591.
[14] Georgiades, P., Watkins, M., Surani, M.A. and Ferguson-Smith, A.C. (2000) Parental origin-specific developmental defects in mice with uniparental disomy for chromosome 12. Development 127, 4719–4728.
[15] Burns, J.L. and Hassan, A.B. (2001) Cell survival and proliferation are modified by insulin-like growth factor 2 between days 9 and 10 of mouse gestation. Development 128, 3819–3830.
[16] Baker, J., Liu, J.P., Robertson, E.J. and Efstratiadis, A. (1993) Role of insulin-like growth factors in embryonic and postnatal growth. Cell 75, 73–82.
[17] Wan, H., Xu, Y., Ikegami, M., Stahlman, M.T., Kaestner, K.H., Ang, S.L. and Whitsett, J.A. (2004) Foxa2 is required for transition to air breathing at birth. Proc. Natl. Acad. Sci. USA 101, 14449–14454.
[18] da Rocha, S.T., Tevendale, M., Knowles, E., Takada, S., Watkins, M. and Ferguson-Smith, A.C. (2007) Restricted co-expression of Dlk1 and the reciprocally imprinted non-coding RNA, Gtl2: implications for *cis*-acting control. Dev. Biol. 306, 810–823.
[19] Hao, Y., Crenshaw, T., Moulton, T., Newcomb, E. and Tycko, B. (1993) Tumour-suppressor activity of H19 RNA. Nature 365, 764–767.
[20] Gabory, A., Ripoche, M.A., Yoshimizu, T. and Dandolo, L. (2006) The H19 gene: regulation and function of a non-coding RNA. Cytogenet. Genome Res. 113, 188–193.
[21] Milligan, L., Antoine, E., Bisbal, C., Weber, M., Brunel, C., Forne, T. and Cathala, G. (2000) H19 gene expression is up-regulated exclusively by stabilization of the RNA during muscle cell differentiation. Oncogene 19, 5810–5816.
[22] Pachnis, V., Brannan, C.I. and Tilghman, S.M. (1988) The structure and expression of a novel gene activated in early mouse embryogenesis. EMBO J. 7, 673–681.
[23] Ripoche, M.A., Kress, C., Poirier, F. and Dandolo, L. (1997) Deletion of the H19 transcription unit reveals the existence of a putative imprinting control element. Genes Dev. 11, 1596–1604.
[24] Ainscough, J.F., Koide, T., Tada, M., Barton, S. and Surani, M.A. (1997) Imprinting of Igf2 and H19 from a 130 kb YAC transgene. Development 124, 3621–3632.
[25] Kawahara, M., Wu, Q., Yaguchi, Y., Ferguson-Smith, A.C. and Kono, T. (2006) Complementary roles of genes regulated by two paternally methylated imprinted regions on chromosomes 7 and 12 in mouse placentation. Hum. Mol. Genet. 15, 2869–2879.